

# Nodal structure of chaotic eigenfunctions

W E Bies<sup>1</sup> and E J Heller<sup>2</sup>

<sup>1</sup> Department of Physics, Harvard University, Cambridge, MA 02138, USA

<sup>2</sup> Department of Physics and Department of Chemistry, Harvard University, Cambridge, MA 02138, USA

Received 31 January 2002, in final form 10 May 2002

Published 28 June 2002

Online at [stacks.iop.org/JPhysA/35/5673](http://stacks.iop.org/JPhysA/35/5673)

## Abstract

We investigate the distribution of nodes at and beyond the classical turning point of idealized chaotic quantum eigenfunctions. A formula for the density of nodes is derived in the semiclassical limit, and the rate at which this density falls off as one moves into the forbidden region is also studied. The discussion is supported by numerical results. Corrections to the Bessel function correlation in the classically allowed region are necessary for finite  $\hbar$  and are given here.

PACS numbers: 03.65.–w, 03.65.Sq, 05.45.Mt

## 1. Introduction

The nature of eigenfunctions of classically chaotic systems has been of considerable interest over the years [1–3]. The statistics, correlations, amplitude and nodal structure of such eigenfunctions have come under study. Random matrix theory and Berry's conjecture suggest that, locally, eigenfunctions of chaotic systems should be random superpositions of plane waves of fixed wavevector magnitude. This implies Gaussian statistics and Bessel function autocorrelations of the resulting random waves.

The nodal structure is of more than academic interest. In many quantum systems in more than one dimension, the presence or absence of nodes of the wavefunction near the classical turning point can control tunnelling rates. For instance, consider tunnelling out of a metastable well in two dimensions [4, 5]. If the wavefunction should have a node at the turning point near the place where the barrier is smallest, the amplitude for tunnelling out will be significantly suppressed relative to the typical case where there is no node, as long as  $\hbar$  is not too small. In fact, tunnelling takes place only within a region of order  $\sqrt{\hbar}$  of the optimal tunnelling path, where the action for crossing the barrier is smallest, and, as will follow from results below, the number of wavelengths within that region scales as only  $\hbar^{-1/6}$ ; thus, for values of  $\hbar$  that one can hope to achieve in numerical experiments the presence or absence of an additional node at the turning point can be important in determining the overall tunnelling rate. Physical processes in which the density of nodes near the turning point is important for the decay rate include for

example photodissociation of molecules and nuclear fission following on absorption of a slow neutron.

The structure of chaotic wavefunctions in the allowed region has also been studied in recent years for disordered systems, where one considers a quantum billiard in the ballistic regime with diffusive surface scattering (see, for instance, the review paper of Mirlin [6]). In addition, Bogomolny and Schmit [7] have obtained analytical results on the distribution of nodal domains for Gaussian random functions.

The structure of chaotic wavefunctions far into the classically allowed region is well understood. As suggested by Berry [8], the wavefunction may be well represented locally by a random superposition of plane waves with fixed wavenumber  $k = (1/\hbar)\sqrt{E - V(x, y)}$ , assuming that  $(x, y)$  does not lie near any short periodic orbits allowing neglect of scarring effects [1]. In such a case, the two-point correlation function  $\langle \psi(\mathbf{x})\psi(\mathbf{x} + \mathbf{r}) \rangle$  is given by  $J_0(kr)$  (see [9]), from which we deduce that the spacing between nodes at  $(x, y)$  is of order  $1/k$ . The generalization to higher dimensions is given in [10]. However, as the turning point is approached, the wavelength diverges and the semiclassical limit breaks down. Nevertheless, as numerical calculations show, there is a finite density of nodes at the turning point which persists, moreover, at least some distance into the forbidden region. This paper provides a theory of the local nodal density in and near the classically forbidden regions, including corrections to local Bessel function correlations in the classically allowed regime.

At first thought, the issue of nodal structure near the turning point surface (i.e. the surface  $V = E$  of zero kinetic energy) and beyond, into the classically forbidden region, seems off limits to semiclassical analysis. However, it is well known that WKB methods are valid deep into forbidden regions, and break down only near singularities in the classical probability densities (e.g. turning points). Even there, connection formulae exist to uniformize the semiclassical methods. Thus, the important question of nodal structure might be addressed after all, at and beyond the  $V = E$  equipotential.

One might imagine that Berry's idea of random superpositions of plane waves simply extends to classically forbidden regions, after replacing sinusoidal waves with appropriate evanescent waves. Consider the kinetic energy  $T$ , for two dimensions,

$$T = p_x^2/2 + p_y^2/2. \quad (1)$$

Even in classically allowed regions, where  $T$  is positive, one may choose for example  $p_x^2$  to be negative, making up the difference with  $p_y^2$ . If this is done, the wave is evanescent in  $x$  and oscillating faster than the nominal wavelength in  $y$ . This is exactly the kind of behaviour we require near diffractive structures whose scale is less than a wavelength. Since evanescent waves blow up in some directions, it is not possible to use them in open systems with no nearby boundaries. But, if boundaries are present, such evanescent waves should (or could) play a role. Complicating this issue is the fact that such evanescent waves can in fact be represented with somewhat pathological linear combinations of travelling waves, as discussed by Berry [11].

In the forbidden regime, the waves must be evanescent in some direction, since  $T$  is negative. One thought towards extending chaotic eigenstates into the forbidden region might be to generalize the idea of random superposition of plane waves to include the evanescent waves in the random sum. This immediately runs into trouble: without any specified boundary condition, runaway (exponentially large) solutions abound. Essentially there is no metric. Furthermore, the idea that the wave amplitude emanates from the classically allowed (albeit chaotic) region would be lost in such a random sum of evanescent waves. The conclusion is that the forbidden regime has to be carefully extended from the allowed region, where the guiding principle is Berry's random superposition of travelling waves deep in classically allowed regions.

What might we expect to be the behaviour of nodal lines at and beyond the turning point surface? Certainly the answer to this question has to depend on the nature of the potential. For a hard-walled billiard, the question is almost moot, but we can expect things to be not radically different for a steep but finite-sloped wall, which does fall in the class of systems we wish to study. The persistence of nodal lines (at the usual density for a free particle of given energy) proximate to a hard wall is well known. The wall, which is itself a nodal line, necessarily intersects interior nodal lines at right angles (as any nodal lines which meet must do).

For a potential which remains bounded but increases beyond the classically allowed region, persistence of any nodes at infinite distances is perhaps surprising. In a sense, a wavefunction with nodes in the forbidden region is not executing an optimal penetration.  $T$  is very negative deep in the forbidden region. Without loss of generality, suppose  $x$  is the direction of steepest ascent, and there are nodal lines locally at  $y = \text{const}_1, \text{const}_2, \dots$ . This implies a locally positive  $p_y^2/2$  in  $T = p_x^2/2 + p_y^2/2$ , making  $p_x^2/2$  more negative, and  $p_x$  larger imaginary. Then the semiclassical penetration integral which goes like

$$\sim \exp\left[-\int^x |p_x(x, y)| dx\right] \quad (2)$$

is attenuating faster than it would if  $p_y = 0$ . In a kind of survival of the fittest, one might expect that such waves would perish compared to others which have no nodes to cause more rapid attenuation.

Against this argument is the notion that the allowed region ‘launches’ waves into the forbidden zone, and it has no interest so to speak in launching optimal penetrating waves. Assuming a variety of waves are launched into the forbidden region, the ‘survival of the fittest’ argument suggests that the nodal density will decrease at some rate as we go deeper into the forbidden region, as the waves with fewer nodes manage to penetrate more easily and start to dominate. This argument necessitates a region of pinching off of nodal lines, as two lines from different places on the turning point surface meet.

The guiding principle of our investigation is to follow typical random waves living in the allowed regions as they make their way into forbidden ones. This is accomplished first with the model introduced next, in the case of one type of potential energy surface.

## 2. Random degenerate harmonic oscillator model

We introduce a very useful generalization of the plane wave superposition which immediately accomplishes the goal of a logical continuation of Berry’s guiding idea into the turning point regime and beyond.

Let the kinetic energy be as above, and the potential energy be  $V(x, y) = x^2 + y^2$ . The  $n$ th level will be  $(n + 1)$ -fold degenerate, spanned by  $\psi_{n,k}(x, y) = \frac{1}{\sqrt{k!(n-k)!}} H_k(x) H_{n-k}(y)$  for  $k = 0, \dots, n$ . Here, we disregard the exponential part of the harmonic oscillator wavefunction because it does not affect where the nodes are. If  $n$  is large, we have a large number of waves  $\psi_{n,k}(x, y)$ ,  $k = 0, \dots, n$ , and we can superpose with random coefficients to make a random degenerate harmonic oscillator eigenfunction:  $\psi = \sum_{k=0}^n a_k \psi_{n,k}$ , where the  $a_k$  are independent identically distributed Gaussian random variables. We stress that the resulting wavefunctions are eigenstates, and are locally random superpositions of plane waves deep in the allowed regions of the potential.

The nodal structure of such a typical wavefunction for  $n = 30$  is shown in figure 1. Note that the wavefunction is symmetric under rotation by  $180^\circ$ . As illustrated in figure 1, the plane is divided generically into three regions: an allowed region where the wavefunction

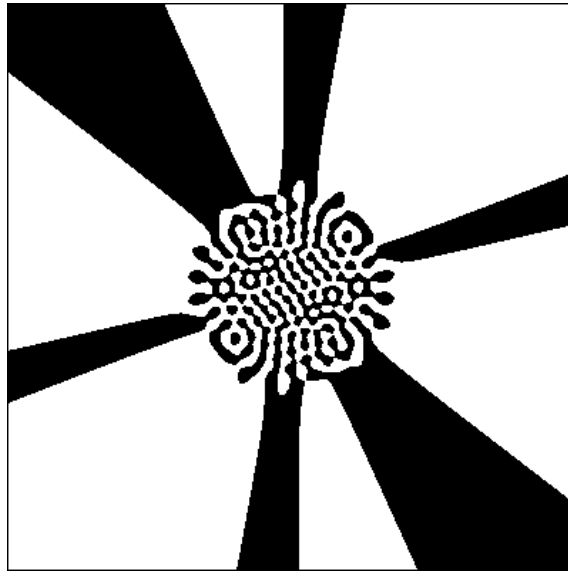


**Figure 1.** Random combination of degenerate two-dimensional harmonic oscillator wavefunctions with  $n = 30$ . White stands for  $\psi > 0$  and black for  $\psi < 0$ . The  $x$ - and  $y$ -axes run from  $-20$  to  $20$ .

is oscillatory, an intermediate region where some nodal lines pinch off, and a forbidden region where a finite number of radial nodal lines tends to infinity. The number of nodal lines persisting to infinity can be deduced by going to polar coordinates  $(x, y) \rightarrow (r, \theta)$ , and expanding the Hermite function  $H_k(r \cos \theta)H_{n-k}(r \sin \theta)$ , keeping the terms of largest order in  $r$ , namely  $r^n$ . These will dominate the random sum as  $r \rightarrow \infty$ . Thus the nodes are determined by the zeros, as a function of  $\theta$ , of the leading term of order  $r^n$ , which is  $\psi = r^n \sum_{k=0}^n a_k c_k c_{n-k} (\cos \theta)^k (\sin \theta)^{n-k}$ , where  $c_k = 1/\sqrt{2^k k!}$ .

A major result for this model is that the number of angular nodes persisting to infinity scales as  $n^{1/2}$ . This can be seen by the following argument. Let  $f_k(\theta) = c_k c_{n-k} (\cos \theta)^k (\sin \theta)^{n-k}$ . This function has four maxima in the interval  $0 < \theta < 2\pi$ , separated on average by  $\pi/2$  radians; the width of the peaks goes as  $n^{-1/2}$ . Now in the correlation function

$$\langle \psi(\theta) \psi(\theta + \Delta\theta) \rangle = \sum_{k=0}^n \langle a_k^2 \rangle f_k(\theta) f_k(\theta + \Delta\theta) \quad (3)$$

we need  $\Delta\theta \sim n^{-1/2}$  for  $f_k$  to decorrelate from itself, independent of  $k$ ; thus, the first zero is expected at a distance  $\Delta\theta \sim n^{-1/2}$  and so the density of zeros (or number of radial lines) must scale as  $n^{1/2}$ . The transition from the regime of radial lines to the pinching-off regime occurs when the subleading term ( $O(r^{n-1})$ ) becomes large enough to compete with the leading term ( $O(r^n)$ ). The former has twice as many terms as the latter, so, assuming random coefficients, we expect the transition to take place around  $\sqrt{2}$  times the radius of the turning point. This defines the pinching region. The number of nodes per unit length on a circle of radius  $r$  clearly decreases from its value at the turning point as one enters the pinching region and falls as  $1/r$  for large  $r$ . We now seek to study these phenomena for a general two-dimensional potential.

### 3. Analysis of nodes near the turning point

The number of nodes in an arbitrary two-dimensional potential which is always increasing as one moves away from the origin can be determined up to a numerical coefficient by

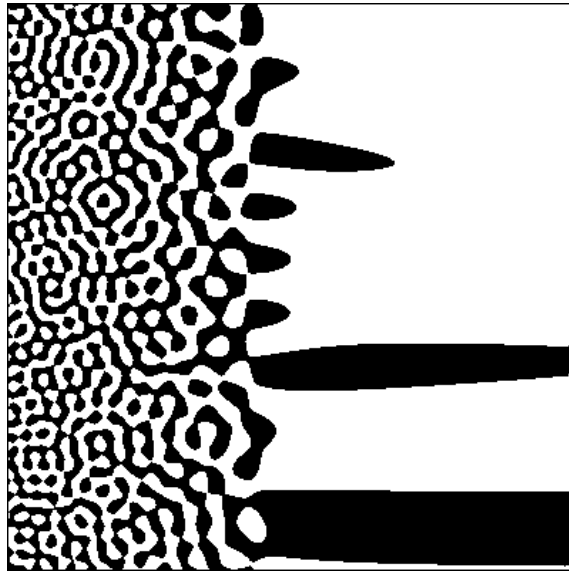


**Figure 2.** Random combination of Airy functions in  $x$  times cosine waves in  $y$ . White stands for  $\psi > 0$  and black for  $\psi < 0$ . The  $x$ - and  $y$ -axes run from  $-25$  to  $25$ .

dimensional analysis. We consider an eigenfunction with energy  $E$  in a two-dimensional potential  $V(x, y)$ . In the semiclassical limit we can approximate the potential near the turning point by a linear-ramp potential; without loss of generality, we can write  $V(x, y) = Cx$  where the equipotential of energy  $E$  is the line  $(x = 0, y)$ .

Thus, near the turning point in the semiclassical limit, the Schrödinger equation separates and the eigenfunction may be written as a superposition of terms of the form

$$\psi_k(x, y) = \text{Ai}\left(\left(C^{1/3}/\hbar^{2/3}\right)(x + \hbar^2 k^2/C)\right) \cos(ky + \delta_k) \quad (4)$$

where  $k$  is the wavevector in the transverse ( $y$ ) direction and  $\delta_k$  is a  $k$ -dependent phase shift. An example of such a superposition is shown in figure 2. The spacing between nodes in the  $x$ -direction is determined by the distance over which the argument of the Airy function changes by an amount of order unity:  $\Delta x \approx \hbar^{2/3}/C^{1/3}$ . We now argue that the spacing of the nodes in the transverse direction is of the same order of magnitude:  $\Delta y \approx \Delta x$ . The reason for this is basically dimensional analysis; there is no other length scale in the problem, so we cannot expect the transverse oscillations to differ systematically in magnitude from the oscillations in the  $x$ -direction. In our problem we can neglect scarring because the fraction of phase space affected by scars on the short periodic orbits vanishes in the semiclassical limit. Therefore, we find that the density of nodes along the equipotential surface  $V(x, y) = E$  is given by  $1/\Delta y$ , or

$$\frac{\#(\text{nodes})}{\text{unit length}} \propto \hbar^{-2/3} |\text{grad}V|^{1/3}. \quad (5)$$

This result is valid only within the limits of the semiclassical analysis. The linearizable region around the turning point must be large enough to cover many wavelengths. For a given potential with a finite slope  $C$  this will be true for sufficiently small  $\hbar$ . We cannot investigate potentials for which the slope at the turning point is infinite nor can we take the limit as the slope  $C$  tends to infinity for fixed  $\hbar$  (as one might want to do for approximating a hard-wall potential).

In order to determine the numerical coefficient in the estimate of the nodal density, we consider the two-point correlation function near the turning point. An arbitrary wavefunction of energy  $E = 0$  will be represented by  $\psi = \int dk a(k)\psi_k$ , where  $a(k)$  are independent Gaussian random variables. We assume that every  $\psi_k$  is derived from a random superposition of plane waves (with random phase shifts) far into the allowed region which is then extrapolated to  $x$  near the turning point (i.e.  $|x|/(\hbar^{2/3}/C^{1/3}) = O(1)$ ) using the Airy function. This has the consequence that at  $x = 0$  any  $\psi_k$  with  $k > 0$  will be exponentially suppressed for large  $k$  due to the fact that the Airy function in equation (4) is in the evanescent region at  $x = 0$  for any  $k > 0$ . The two-point correlation function is then given by

$$C(x, y; x', y') = \langle \psi(x, y)\bar{\psi}(x', y') \rangle \quad (6)$$

$$= \int dk \cos k(y - y') \quad (7)$$

$$\times \text{Ai}\left(\frac{C^{1/3}}{\hbar^{2/3}}(x + \hbar^2 k^2/C)\right) \quad (8)$$

$$\times \text{Ai}\left(\frac{C^{1/3}}{\hbar^{2/3}}(x' + \hbar^2 k^2/C)\right). \quad (9)$$

The two-point correlation function  $C(0, 0; 0, y)$  as a function of  $y$  is oscillatory and damped, similar to the Bessel function which is valid in the allowed region but with a more rapid decay at large  $y$ . From its first zero we infer a nodal density of 0.19 on the line  $x = 0$ , in comparison with the numerical value of 0.16, which was obtained by counting the zeros of an ensemble of wavefunctions with random coefficients of the  $\psi_k$  in equation (4). This number is the numerical coefficient in equation (5). Away from the turning point in the allowed region, the Airy function in  $\psi_k$  is approximately sinusoidal near a given point, with a definite phase depending on  $k$ . Thus,  $\psi_k$  looks locally like a combination of plane waves. For  $x$  far into the allowed region (i.e.  $|x|$  not small compared to the radius of curvature of the  $V = 0$  equipotential at  $(x, y) = (0, 0)$ ) the separability assumption underlying equation (4) breaks down for a general potential. Then plane waves with arbitrary phases, not just those contained in equation (4), will be present and the Bessel function correlation  $J_0(kr)$  of [9] is recovered.

Berry found the exact value of the nodal density at the turning point to be 0.17099 (see the appendix).

#### 4. Analysis of nodes in the forbidden region

We now study the pinching of nodes in the forbidden region, first for the linear-ramp potential. Let  $P_x(k)$  denote the distribution of transverse momenta at  $x > 0$ . The idea is that the higher-frequency components in  $\psi$  die off more rapidly than the lower-frequency ones, leading to a compression of the support of  $P_x(k)$ , hence smaller  $\langle k \rangle_x = \int k P_x(k) dk$  and hence a larger nodal spacing as  $x$  increases. We employ the asymptotic expansion of the Airy function for large  $x$ :

$$P_x(k) = \left\langle \left| \int dy e^{-iky} \psi(x, y) \right|^2 \right\rangle \quad (10)$$

$$= \text{Ai}\left(\frac{C^{1/3}}{\hbar^{2/3}}(x + \hbar^2 k^2/C)\right)^2 \quad (11)$$

$$\approx \frac{1}{4} \frac{1}{(C^{1/3}/\hbar^{2/3}) (x + \hbar^2 k^2/C)^{1/2}} \exp\left(-\frac{4}{3} \frac{C^{1/2}}{\hbar} |x + \hbar^2 k^2/C|^{3/2}\right) \tag{12}$$

$$\approx (\text{const}) e^{-(k/k_x)^2} \tag{13}$$

where we expand the argument of the exponential yielding  $|x|^{3/2} + \frac{3}{2}x^{1/2}\hbar^2 k^2/C$  and then we set  $k_x = C^{1/4}/2^{1/2}\hbar^{1/2}x^{1/4}$ . The denominator in equation (12) can be treated as nearly independent of  $k$  for sufficiently large  $x$ , since the whole expression is exponentially suppressed for  $k \gg k_x$  but  $\hbar^2 k^2/C \ll x$ . In the last line the factor  $k_x$  just rescales the  $k$ -distribution by an amount depending on  $x$ . In the same approximation the wavefunction is given up to a constant by

$$\psi(x, y) = \int dk a(k) e^{-k^2/2k_x^2} \cos(ky + \delta_k) \tag{14}$$

$$= \int dk' a(k_x k') e^{-k'^2/2} \cos(k' y' + \delta_{k,k'}) \tag{15}$$

$$= \int dk' a(k') e^{-k'^2/2} \cos(k' y' + \delta_{k'}) \tag{16}$$

with  $k' = k/k_x$  and  $y' = k_x y$ . The equality between the second and third lines holds in a statistical sense, which is all we are concerned with here; since the  $a$  and  $\delta$  are independent identically distributed random variables, relabelling them does not affect the statistical properties of  $\psi(x, y)$ . Then from equation (16) we see that  $\psi(x_1, y)$  and  $\psi(x_2, y)$  have the same form up to a rescaling in the  $y$ -direction. Apart from the linear rescaling of  $y$  by the factor  $k_x$ , the number of zeros in the  $y$ -direction at fixed  $x$  depends only on the  $x$ -independent form of  $\psi(x, y)$  in equation (16). Therefore, the nodal density must scale as  $x^{-1/4}$  for large  $x$ . This analytical result is in agreement to within 2% with numerical results for random wavefunctions of the type given in equation (4). It is also in agreement with the expression given above for the two-point correlation function in the forbidden region; i.e. the first zero  $y(x)$  of  $C(x, 0; x, y)$  as a function of  $x > 0$  scales as  $x^{1/4}$  for large  $x$ . The most direct evidence confirming the  $x^{-1/4}$ -dependence of the nodal density was obtained by solving for high-lying eigenfunctions in an ensemble of chaotic two-dimensional Hamiltonians and counting the average number of zeros on energy equipotentials of increasing radius. The potential used was of the form  $V(x, y) = x^2 + y^2 + \lambda x^2 y^2$  with  $\lambda = 0.1$  plus a number of Gaussian bumps with random heights and positions in the classically allowed region. Numerically we were able to generate eigenfunctions that had five to six wavelengths across the classically allowed region, far enough into the semiclassical regime that the  $x^{-1/4}$ -dependence should be expected. As shown in figure 3, the numerical results for the nodal density are approximately given by an  $x^{-1/4}$  law for radii greater than 6 (the numerical exponent is close to  $-0.30$ ). The derivation of the  $x^{-1/4}$ -dependence breaks down near the turning point at radius 5.5. Near the turning point, the nodal density approaches a constant value of 0.37, which is to be compared with the prediction of equation (5) using the numerical value of the constant of proportionality, namely 0.16. Equation (5) yields a predicted nodal density at the turning point of 0.40. The slight discrepancy with the computed value is probably due to the fact that the radius of curvature of the equipotential at the turning point was not large compared to the nodal spacing, as was assumed in the semiclassical derivation. According to Berry (see the appendix), the nodal density tends to  $1/2\pi x^{1/4}$  for sufficiently large  $x$ . At radius 6.5, corresponding to  $x = 1$ , the nodal density is about twice what the asymptotic formula predicts. The faster fall off in figure 3 with an exponent of  $-0.30$ , slightly greater than  $-0.25$ , presumably continues until the asymptotic form is reached. At radii larger than the upper end of the range plotted in figure 3 the nodal density cannot be computed due to numerical noise.

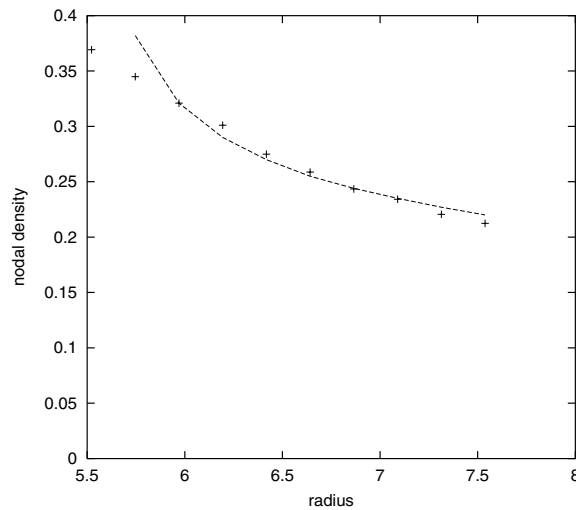


**Figure 3.** Nodal density for chaotic eigenfunctions near energy  $E = 15.25$  (the 100th state from the bottom of the well) arising from a potential consisting of  $V(x, y) = x^2 + y^2 + \lambda x^2 y^2$  plus random Gaussians in the allowed region, with  $\lambda = 0.1$ , plotted versus radius (distance along the  $x$ -axis from the origin to the equipotential  $V = E$ ). Crosses indicate numerical results and the dashed line the theoretically predicted  $x^{-1/4}$  fall off.

Very recently, Berry was able to verify the asymptotic  $x^{-1/4}$ -dependence by deriving an analytic expression for the nodal density that reduces to an  $x^{-1/4}$ -dependence far into the forbidden region (see the appendix).

We can generalize this result to potentials with non-linear  $x$ -dependence but no  $y$ -dependence, i.e.  $V(x, y) = V(x)$ . Then the semiclassical propagator implies that  $\psi_k$  decays in the forbidden region as follows:

$$\psi_k = \left| \frac{\partial^2 S(x, E)}{\partial x \partial E} \right|^{1/2} e^{-|S(x, E)/\hbar|} \quad (17)$$

with  $E = -k^2$  (so that the total energy is zero) and  $S(x, E)$  the action of the path with energy  $E$  that goes from the turning point along the  $x$ -axis to the point  $(x, 0)$ . The prefactor is given by  $(\sqrt{V(x) + k^2})^{-1/4}$  while the argument of the exponential is  $\int_0^x dx \sqrt{V(x) + k^2}$ . The  $k$ -dependence of the change in the argument of the exponential with  $x$  is given by  $\sqrt{V(x) + k^2} - \sqrt{V(x)}$  which to leading order for large  $x$  is just  $k^2/2\sqrt{V(x)}$ . Thus as before the distribution in  $k$  becomes narrower as one goes farther into the forbidden region. The width in  $k$  scales as  $1/\sqrt{\int^x dx/\sqrt{V(x)}}$ . Interestingly, this implies that the distribution in  $k$  becomes stationary in  $x$  for large  $x$  if the potential grows rapidly enough; i.e.  $V(x) = (\text{const})x^\alpha$  with  $\alpha > 2$ . An intuitive physical explanation of this result would be helpful, but we have not found one so far. This analysis fails for any realistic potential with finite radius of curvature of the equipotential through the turning point. The typical wavevector at the turning point scales as  $\hbar^{-2/3}$ ; in the semiclassical limit the distance one has to go into the forbidden region for  $k^2 \ll V(x)$  tends to infinity and the assumption that the potential is independent of  $y$  breaks down.

## 5. Transition to semiclassical behaviour in the allowed region

Far into the classically allowed region the wavefunction near  $(x_0, 0)$  may be written as a random sum of plane waves:

$$\psi(x, y) = \int d\theta a_\theta \exp(-i(k_0(\cos \theta, \sin \theta) \cdot (\mathbf{x} - \mathbf{x}_0) + \delta_\theta)) \tag{18}$$

where  $k_0 = (1/\hbar)\sqrt{E - V(x_0, 0)}$  and  $a_\theta$  are independent identically distributed Gaussian random variables; i.e.  $\langle a_\theta a_{\theta'} \rangle = \delta(\theta - \theta')$ . The phase shifts  $\delta_\theta$  are also assumed independent and uniformly distributed on the interval  $[0, 2\pi]$ . We call this the circular distribution. In order to compare with the behaviour of the wavefunction for  $x_0 < x < 0$  we compute the normalized probability distribution for the transverse momentum:

$$P_{x_0}(k_y) = \left\langle \left| \int dy e^{-ik_y y} \psi(x_0, y) \right|^2 \right\rangle. \tag{19}$$

Substituting from equation (18) we have

$$P_{x_0}(k_y) = \left\langle \int dy dy' d\theta d\theta' a_\theta a_{\theta'} \exp(i(k_y y - k_y y' - \mathbf{k}_\theta \cdot (x_0, y) + \mathbf{k}_{\theta'} \cdot (x_0, y') + \delta_\theta - \delta_{\theta'})) \right\rangle. \tag{20}$$

The ensemble average over the phase shifts yields a  $\delta(\theta - \theta')$ . Then the ensemble average over the  $a_\theta$  reduces to  $\langle a_\theta^2 \rangle = 1$ . The integrand in equation (20) becomes

$$P_{x_0}(k_y) = \int dy dy' d\theta e^{i(k_y - k_0 \sin \theta)(y - y')} \tag{21}$$

$$= \int d\theta \delta(k_y - k_0 \sin \theta) \tag{22}$$

$$= \frac{(2/\pi)}{\sqrt{k_0^2 - k_y^2}} \Theta(k_y - k_0). \tag{23}$$

In the last step we have normalized such that  $\int_0^\infty dk_y P_{x_0}(k_y) = 1$ . Near the turning point, however, we saw above that  $P_0(k_y) = \text{Ai}(\hbar^{4/3} k_y^2 / C^{2/3})^2$ . Clearly there must be a transition region between this result for  $x = 0$  and the circular distribution (equation (23)) for  $x = x_0 < 0$  far enough into the allowed region for the semiclassical limit to apply. In the limit as  $\hbar$  tends to zero for a given potential  $V(x, y)$  the semiclassical limit will be attained for  $x_0 < 0$  still lying in the linearizable region of the potential around the turning point; therefore, we can restrict our attention to the case  $V(x, y) = Cx$ . For simplicity, let us adopt units such that  $\hbar = C = 1$ .

The presence of the classical turning point modifies the form of the plane waves that are allowed in the region near it. For the case of a hard-walled billiard, this issue has been the subject of a recent investigation by Berry [12]. If, for example, there were a hard wall at  $x = 0$ , one would have to exclude plane waves that did not vanish at  $x = 0$ . This can be done by subtracting the reflected wave from the incident wave. The most general allowed plane waves in the case of a hard wall are thus of the form  $e^{-ik_y y + i\delta} \sin k_x x$  with  $k_x^2 + k_y^2 = k^2$ . In a billiard with an irregularly shaped boundary this ensemble of plane waves will go over to the circular ensemble when the distance to the wall is not small compared to the radius of curvature of the boundary. Similarly in the case of a ramp potential the most general plane wave near the turning point is of the form

$$e^{-ik_y y + i\delta} \sin(k_x x + \delta_{x, k_y}) \tag{24}$$

where  $k_x^2 + k_y^2 = k^2 = |x|$  and  $\delta_{x, k_y}$  is a phase shift that ensures that the sine wave is in phase with  $\text{Ai}(x + k_y^2)$  at the point  $(x, 0)$ . The exclusion of all other plane waves can be understood from the following argument. A sine wave with arbitrary phase at a given point

$x < 0$  can be represented locally as a combination of the Airy function  $\text{Ai}(x + k_y^2)$  and the complementary Airy function  $\text{Ai}'(x + k_y^2)$ . These can now be extrapolated to  $x$  near the turning point. However, the complementary Airy function diverges when its argument is greater than zero, i.e. for  $x > -k_y^2$ . Therefore we must impose the physical requirement that the coefficient of the complementary Airy function be zero, and this is done by choosing the phase  $\delta_{x,k_y}$  so that the sine wave is in phase with the Airy function.

We start with a wavefunction which is a random superposition of plane waves of the form given in equation (24):

$$\psi(x, y) = \int d\theta a_\theta e^{-ik_0 \sin \theta y + i\delta_\theta} \sin(k_0 \cos \theta x + \delta_{x,k_0 \sin \theta}) \tag{25}$$

and then match the sine waves in  $x$  to Airy functions which have the same rate of oscillation near  $x = x_0$ . The matching is given by

$$e^{-ik_y y + i\delta} \sin(k_x x + \delta_{x,k_y}) \approx \frac{\text{Ai}(x + k_y^2)}{\text{Ae}(x_0 + k_y^2)} e^{-ik_y y + i\delta} \tag{26}$$

near  $x = x_0$ , with  $k_y = k_0 \sin \theta$ . We have introduced the Airy envelope function, denoted by  $\text{Ae}$ . For  $x < x_{\text{max}}$  it is given approximately by  $1/\sqrt{\pi}|x|^{1/4}$ ,  $x_{\text{max}} = -1.0188$  being the position of the first maximum of the Airy function for  $x < 0$ , and for  $x > x_{\text{max}}$ , where the Airy function is no longer oscillatory, we set  $\text{Ae}(x) = \text{Ai}(x)$ . Thus,  $\psi(x, y)$  is known in the region  $x_0 < x < 0$  by substitution of equation (26) into equation (25). Now  $\psi(x, y)$  can be extrapolated from  $x = x_0$  to a point closer to the turning point  $x = x_1$  with  $x_0 < x_1 < 0$ . If we assume  $|x_1| \ll |x_0|$  the Airy envelope function in the denominator becomes approximately constant for  $k < |x_1|^{1/2}$ ; the Airy function in the numerator is exponentially damped for  $k > |x_1|^{1/2}$ . The wavefunction, equation (25), can be written with the aid of the matching formula, equation (26), as follows:

$$\psi(x, y) \approx \int d\theta a_\theta \frac{\text{Ai}(x + k_{\theta y}^2)}{\text{Ae}(x_0 + k_{\theta y}^2)} e^{-ik_{\theta y} y + i\delta_\theta} \tag{27}$$

The distribution at  $x_0$  can be extrapolated to the distribution at  $x_1 < 0$  with  $|x_1| \ll |x_0|$  by means of equation (27):

$$P_{x_1}(k_y) = \left\langle \left| \int dy e^{-ik_y y} \psi(x_1, y) \right|^2 \right\rangle \tag{28}$$

$$= \left\langle \int dy dy' d\theta d\theta' a_\theta a_{\theta'} \frac{\text{Ai}(x_1 + k_{\theta y}^2) \text{Ai}(x_1 + k_{\theta' y'}^2)}{\text{Ae}(x_0 + k_{\theta y}^2) \text{Ae}(x_0 + k_{\theta' y'}^2)} \right. \tag{29}$$

$$\left. \times \exp(i(k_y(y - y') - k_{\theta y} y + k_{\theta' y'} y' + \delta_\theta - \delta_{\theta'})) \right\rangle \tag{30}$$

Again the ensemble average over the phase shifts yields a  $\delta(\theta - \theta')$ . Then the ensemble average over the  $a_\theta$  reduces to  $\langle a_\theta^2 \rangle = 1$ . We are left with

$$P_{x_1}(k_y) = \int dy dy' d\theta \frac{\text{Ai}(x_1 + k_{\theta y}^2)^2}{\text{Ae}(x_0 + k_{\theta y}^2)^2} e^{i(k_y - k_{\theta y})(y - y')} \tag{31}$$

$$= \int d\theta \frac{\text{Ai}(x_1 + k_{\theta y}^2)^2}{\text{Ae}(x_0 + k_{\theta y}^2)^2} \delta(k_y - k_{\theta y}) \tag{32}$$

$$= \left( \frac{1}{\sqrt{k_0^2 - k_y^2} \operatorname{Ai}(x_0 + k_y^2)} \right) \operatorname{Ai}(x_1 + k_y^2)^2. \tag{33}$$

The prefactor is approximately 1 for  $|x_1| \ll |x_0|$ . This leaves

$$P_{x_1}(k_y) = (\text{const}) \operatorname{Ai}(x_1 + k_y^2)^2 \tag{34}$$

where the  $x_1$ -dependent constant is chosen such that  $\int_0^\infty P_{x_1}(k_y) dk_y = 1$ . This analytical form has the right limiting behaviour; for  $x_1 = 0$  it reduces trivially to the  $P_0(k_y)$  obtained above and for large  $|x_1|$  we see that equation (23) is recovered upon insertion of the asymptotic form of the Airy function. Here, one must average over the rapid oscillations of the Airy function. The oscillations in the momentum distribution  $\operatorname{Ai}(x_1 + k_y^2)^2$  are due to the fact that the Airy functions  $\operatorname{Ai}(x + k_y^2)$  in equation (4) have zeros in the allowed region. At the positions of the zeros, there can be no waves with transverse momentum  $k_y$ . If one goes far enough into the allowed region the circular distribution will be recovered, but for sufficiently small  $\hbar$  there will always be a region near the turning point where equation (34) holds. In figure 4 we show how equation (34) explains the transition from the circular distribution far into the allowed region to the Airy function distribution near the turning point. Because the envelope of the Airy function falls rather slowly ( $\sim |x_1|^{-1/4}$ ) one has to go to rather large  $|x_1| \sim 100$  before  $P_{x_1}(k_y)$  begins to acquire the sharp peak at  $k_y = |x_1|^{1/2}$  characteristic of the circular distribution. For intermediate  $x_1$  the peak is rounded. Finally, we may change units and express  $P_{x_1}(k_y)$  as  $\operatorname{Ai}((C^{1/3}/\hbar^{2/3})(x_1 + \hbar^2 k_y^2/C))^2$ . This shows that the transition region becomes much larger for smaller slopes of the potential at the turning point. To our knowledge, the analytical form (34) expressing the correction to random matrix theory in chaotic wavefunctions near the classical turning point has not been given before in the literature. Our result is important for the numerical calculation of eigenfunctions in smooth potentials. It is doubtful whether one could ever get beyond the transition region, since it is so large in terms of number of wavelengths from the turning point.

### 6. Discussion

In the process of finding the correct nodal density and correlation functions at turning points and beyond, we have found corrections to Berry’s conjecture in the classically allowed region as well. These corrections actually persist rather deep into the allowed region for reasonable values of  $\hbar$ , so that most problems with smooth potentials will nowhere exist in regimes where the corrections can be entirely ignored. Equation (34) shows the transition from the Airy function distribution near the turning point to Berry’s circular distribution as one goes far enough into the classically allowed region.

For distances into the forbidden region on the order of  $\hbar^{2/3}$  we may represent the wavefunction as a superposition of Airy functions and obtain results on the nodal density at the turning point, and on the rate at which the nodal density falls off as one goes into the forbidden region. These will apply so long as the distance into the forbidden region is small compared to the radius of curvature of the energy equipotential at the turning point; this supplies an  $\hbar$ -independent criterion for the breakdown of our results.

It would be desirable to understand how the nodal density behaves at radii large compared to the radius of curvature, but we have not made any progress in this since the separability assumption does not hold in this region.

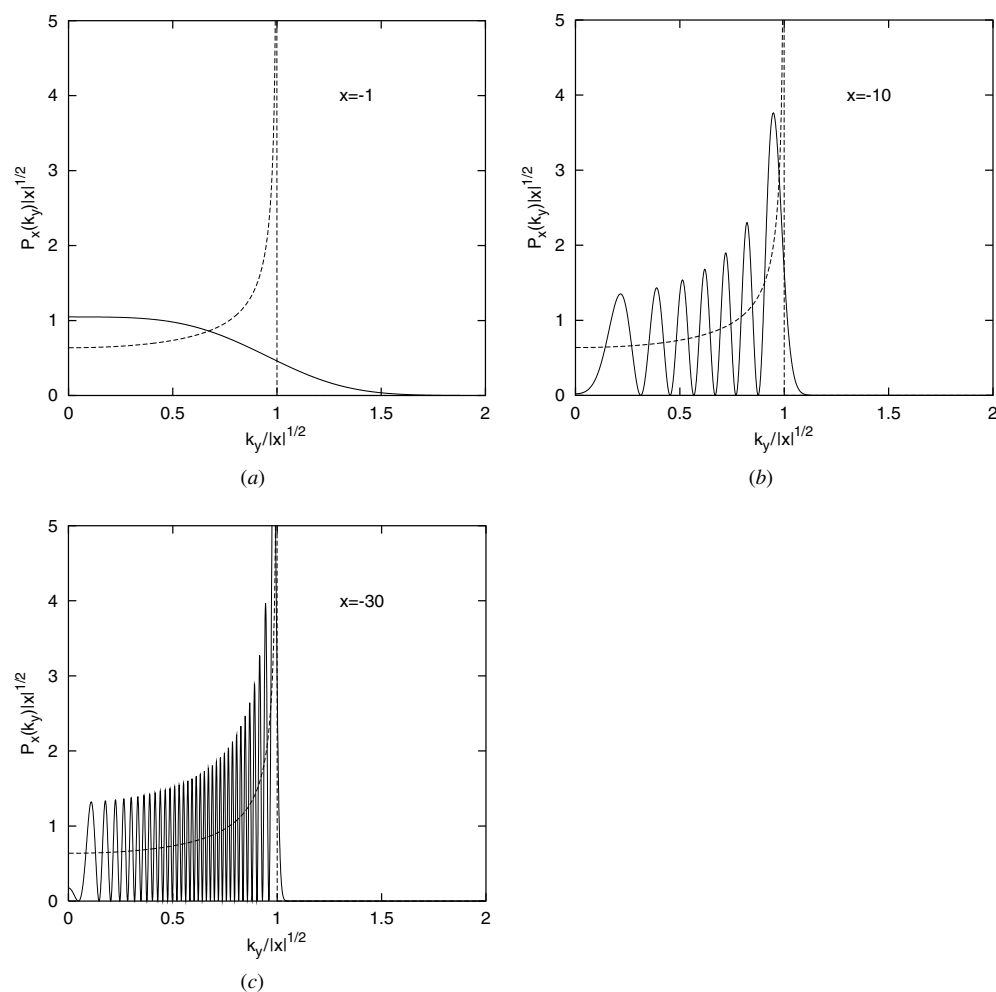


**Figure 4.** Distribution of transverse momenta,  $P_x(k_y)$  (equation (34)), in a chaotic wavefunction near the turning point at  $x = 0$  (in dimensionless units), solid lines, and the circular distribution (equation (23)), dashed lines. (a)  $x = -1$ , (b)  $x = -10$ , (c)  $x = -30$ . At the turning point the two differ greatly, but as  $|x|$  increases the distribution  $P_x(k_y)$  begins to turn over and by  $x = -30$  the envelope of the circular distribution is almost regained.

If the large-radius region could be understood, we would have in principle a complete picture of the statistical properties of generic chaotic wavefunctions (i.e. neglecting scarring) for two-dimensional smooth potentials in the semiclassical limit.

It would also be of interest to investigate nodal-line crossings and modifications of the generic pattern due to scars.

### Acknowledgments

We thank Lev Kaplan for helpful discussions. This work was supported by a grant from the National Science Foundation, NSF CHE-0073544.

## Appendix

In recent work Berry has verified our finding and derived a remarkable analytical expression for the nodal density in the case of a linear-ramp potential, which he has kindly communicated to us [13]. In coordinates  $(X, Y)$  such that the turning point is the line  $Y = 0$ , the nodal density  $\rho_L(Y)$  is given by

$$\rho_L(Y) = \frac{D_x (BD_y - K^2)}{\pi} \int_0^{\pi/2} \frac{d\theta}{(BD_x \cos^2 \theta + (BD_y - K^2) \sin^2 \theta)^{3/2}} \quad (35)$$

where

$$B(Y) = 2 \int_0^\infty dQ \text{Ai}(Y + Q^2)^2 \quad (36)$$

$$D_x(Y) = 2 \int_0^\infty dQ Q^2 \text{Ai}(Y + Q^2)^2 \quad (37)$$

$$D_y(Y) = 2 \int_0^\infty dQ \text{Ai}'(Y + Q^2)^2 \quad (38)$$

and

$$K(Y) = 2 \int_0^\infty dQ \text{Ai}(Y + Q^2) \text{Ai}'(Y + Q^2). \quad (39)$$

This has the asymptotic forms

$$\rho_L(Y) = \begin{cases} \sqrt{|Y|}/2\sqrt{2} & Y \ll 0 \\ 0.17099 & Y = 0 \\ 1/2\pi Y^{1/4} & Y \gg 0 \end{cases} \quad (40)$$

which agree with our predictions for  $Y = 0$  and  $Y \gg 0$ .

## References

- [1] Heller E J 1984 *Phys. Rev. Lett.* **53** 1515
- [2] Schnirelman A I 1974 *Usp. Mat. Nauk* **29** 181 (in Russian)  
Zelditch S 1987 *Duke Math. J.* **55** 919  
Colin de Verdiere Y 1985 *Commun. Math. Phys.* **102** 497  
Voros A 1979 *Springer Lecture Notes in Physics* vol 93 ed G Casati and J Ford (New York: Springer) pp 326–33
- [3] Berry M V 1991 Some quantum-to-classical asymptotics *Les Houches Lecture Series LII (1989)* ed M-J Giannoni, A Voros and J Zinn-Justin (Amsterdam: North-Holland) pp 251–304
- [4] Creagh S C and Whelan N D 1999 *Ann. Phys., NY* **272** 196
- [5] Bies W E, Kaplan L and Heller E J 2001 *Phys. Rev. E* **64** 016204
- [6] Mirlin A 2000 *Phys. Rep.* **326** 259
- [7] Bogomolny E and Schmit C 2002 *Phys. Rev. Lett.* **88** 114102
- [8] Berry M V 1983 *Chaotic Behaviour of Deterministic Systems* ed G Iooss, R Helleman and R Stora (Amsterdam: North-Holland) p 171
- [9] Berry M V 1983 *Ann. NY Acad. Sci.* **357** 183
- [10] Berry M V 1977 *J. Phys. A: Math. Gen.* **10** 2083
- [11] Berry M V 1994 *J. Phys. A: Math. Gen.* **27** L391–8
- [12] Berry M V 2002 *J. Phys. A: Math. Gen.* **35** 3025
- [13] Berry M V 2002 Private communication